The FlhA linker mediates flagellar protein export switching during flagellar assembly

Yumi Inoue[1,†], Mamoru Kida[2], Miki Kinoshita[1], Norihiro Takekawa[2], Keiichi Namba[1,3,4], Katsumi Imada[2,*] and Tohru Minamino[1,*]

[1] Graduate School of Frontier Biosciences, Osaka University, 1-3 Yamadoaka, Suita, Osaka 565-0871, Japan

[2] Department of Macromolecular Science, Graduate School of Science, Osaka University, 1-1 Machikaneyama-cho, Toyonaka, Osaka 560-0043, Japan

[3] RIKEN Spring-8 Center and Center for Biosystems Dynamics Research, 1-3 Yamadaoka, Suita, Osaka 565-0871, Japan

[4] JEOL YOKOGUSHI Research Alliance Laboratories, Osaka University, 1-3 Yamadaoka, Suita, Osaka 565-0871, Japan

[†]Present address: Department of Ophthalmology and Visual Sciences, Kyoto University Graduate School of Medicine, Kyoto, 606-8507 Japan

*Correspondence to Tohru Minamino : Mailing address, Graduate School of Frontier Biosciences, Osaka University, 1-3 Yamadaoka, Suita, Osaka 565-0871, Japan. Tel: +81-6-6879-4625; E-mail: tohru@fbs.osaka-u.ac.jp or Katsumi Imada: Graduate School of Sciences, Osaka University, 1-1 Machikaneyama, Toyonaka, Osaka 560-0043, Japan. Tel: +81-6-6850-5455; E-mail: kimada@chem.sci.osaka-u.ac.jp.

Abstract

The flagellar protein export apparatus switches export specificity from hook-type to filament-type upon completion of hook assembly, thereby initiating filament assembly at the hook tip. The C-terminal cytoplasmic domain of FlhA ($FlhA_C$) forms a homo-nonameric ring structure that serves as a docking platform for flagellar export chaperones in complex with their cognate filament-type substrates. Interactions of the flexible linker of FlhA ($FlhA_L$) with its nearest $FlhA_C$ subunit in the ring allow the chaperones to bind to $FlhA_C$ to facilitate filament-type protein export, but it remains unclear how it occurs. Here, we report that $FlhA_L$ acts as a switch that brings the order to flagellar assembly. The crystal structure of $FlhA_C$(E351A/D356A) showed that Trp-354 in $FlhA_L$ bound to the chaperone-binding site of its neighboring subunit. We propose that $FlhA_L$ binds to the chaperon-binding site of $FlhA_C$ to suppress the interaction between $FlhA_C$ and the chaperones until hook assembly is completed.

Introduction

The flagellum of *Salmonella enterica* (hereafter referred to *Salmonella*) is a supramolecular motility machine consisting of the basal body, the hook and the filament. For construction of the flagella on the cell surface, a type III protein export apparatus (fT3SS) transports flagellar building blocks from the cytoplasm to the distal end of the growing flagellar structure. The fT3SS is divided into three structural parts: a transmembrane export gate complex made of FlhA, FlhB, FliP, FliQ and FliR, a docking platform composed of the cytoplasmic domains of FlhA and FlhB ($FlhA_C$ and $FlhB_C$), and a cytoplasmic ATPase ring complex consisting of FliH, FliI and FliJ[1]. The $FlhA_C$-$FlhB_C$ docking platform switches its substrate specificity from hook-type export substrates (FlgD, FlgE and FliK) to filament-type ones (FlgK, FlgL, FlgM, FliC and FliD) when the hook reaches its mature length of about 55 nm in *Salmonella*, thereby terminating hook assembly and initiating filament formation[2].

FliK is secreted via fT3SS during hook-basal body (HBB) assembly not only to measure the hook length but also to switch export specificity of the $FlhA_C$-$FlhB_C$ docking platform[2]. This has been recently verified by *in vitro* reconstitution experiments using inverted membrane vesicles[3,4]. The N-terminal domain of FliK ($FliK_N$) serves as a secreted molecular ruler to measure the hook length[5–8]. When the hook length reaches about 55 nm, a flexible linker region of FliK connecting $FliK_N$ and the C-terminal domain ($FliK_C$) promotes a conformational rearrangement of $FliK_C$ to interact with $FlhB_C$, thereby

terminating hook-type protein export[9,10].

FlhA$_C$ consists of four domains, D1, D2, D3 and D4, and a flexible linker (FlhA$_L$) connecting FlhA$_C$ with the N-terminal transmembrane domain of FlhA (Fig. 1)[11]. FlhA$_C$ forms a homo-nonamer ring[12,13] and provides binding-sites for flagellar export chaperons (FlgN, FliS and FliT) in complex with their cognate filament-type substrates[14–17]. Interactions of FlhA$_C$ with the flagellar chaperones facilitate the filament-type substrates to enter into the export gate complex for efficient protein export and assembly[15,16]. The FliK$_C$-FlhB$_C$ interaction is thought to induce structural remodeling of the FlhA$_C$ ring through interactions of FlhA$_L$ with its nearest FlhA$_C$ subunit, thereby initiating the export of filament-type proteins[13,18,19]. However, it remains unknown how.

In the present study, to clarify the role of FlhA$_L$ in the export switching mechanism of fT3SS, we analyzed the interaction between FlhA$_L$ and FlhA$_C$ and provide evidence suggesting that the interaction of FlhA$_L$ with the chaperone-binding site of FlhA$_C$ inhibits the binding of the flagellar export chaperones to FlhA$_C$ to keep the export specificity in the hook type during hook assembly.

Results

Isolation of pseudorevertants from the *flhA(E351A/W354A/D356A)* mutant. Glu-351, Trp-354 and Asp-356 of FlhA$_L$ bind to the D1 and D3 domains of its neighboring FlhA$_C$

subunit to stabilize $FlhA_C$ ring structure in solution[11,13]. The *flhA(E351A/D356A)* and *flhA(W354A)* mutants produces the HBBs without the filament attached although their hook length is not controlled properly[13]. The W354A and E351A/D356A mutations inhibit the interaction of $FlhA_C$ with flagellar chaperones in complex with their cognate filament-type substrates, suggesting that the interaction between $FlhA_L$ and the D1 and D3 domains of its neighboring $FlhA_C$ subunit keeps the chaperone binding site of $FlhA_C$ open to allow the chaperones to bind to $FlhA_C$ to facilitate the export of the filament-type substrates[13]. However, the *flhA(E351A/W354A/D356A)* mutant do not produce the HBBs at all, raising a question of why the E351A/W354A/D356A triple mutation inhibits HBB assembly[13]. To clarify this question, we isolated 14 pseudorevertants from the *flhA(E351A/W354A/D356A)* mutant. Motility was somewhat restored by these pseudorevertant mutations but it was much poorer than that of wild-type cells (Fig. 2a). Export substrates such as FlgD, FlgE, FlgK and FliD were detected in the culture supernatants of these pseudorevertants (Fig. 2b). In agreement with this, these pseudorevertants produced a couple of flagella on the cell surface (Fig. 2c). DNA sequencing revealed that all suppressor mutations are located in the *flgMN* operon. One was the M1I mutation at the start codon of the *flgM* gene (isolated twice), presumably inhibiting FlgM translation. Two suppressor mutations produced a stop codon at position of Gln-52 or Ser-85 of FlgM, resulting in truncation of the C-terminal region of FlgM. Nine suppressor mutations were large deletions in *flgM*. We also found that there was a large

99 deletion in the *flgM* and *flgN* genes, thereby disrupting both FlgM and FlgN. A
100 loss-of-function of FlgM results in a considerable increment in the transcription levels of
101 flagellar genes[20,21]. Consistently, the cellular levels of FlgK and FliD seen in the
102 pseudorevertants were higher than those in its parental strain (Fig. 2b, 3rd and 4th rows).
103 It has been shown that an interaction between FliJ and $FlhA_L$ brought about by FliH and
104 FliI fully activates the transmembrane export gate complex of fT3SS to utilize proton
105 motive force (PMF) across the cell membrane to drive flagellar protein export[22]. Because
106 the E351A/W354A/D356A triple mutation reduces the binding affinity of $FlhA_C$ for FliJ[13],
107 this suggests that these *flgM* mutations considerably increase the cytoplasmic levels of
108 FliH, FliI, FliJ and export substrates to allow the *flhA(E351A/W354A/D356A)* mutant to
109 export flagellar building blocks for producing a small number of flagella on the cell
110 surface. Therefore, we propose that Glu-351, Trp-354 and Asp-356 of $FlhA_L$ also play an
111 important role in the activation mechanism of the PMF-driven export gate complex.

112 We found that the secretion levels of FlgD and FlgE by the pseudorevertants
113 were about 1.5-fold and 4-fold higher than those by the wild-type whereas the secretion
114 levels of FlgK and FliD were much lower (Fig. 2b), raising the possibility that *flgM*
115 suppressor mutations do not efficiently promote export switching of fT3SS from
116 hook-type substrates to filament-type ones in the *flhA(E351A/W354A/D356A)* mutant. To
117 clarify this, we introduced the Δ*flgM*::*km* allele to the *Salmonella* NH001 (Δ*flhA)* strain to
118 produce the Δ*flgM*::*km* and *flhA(E351A/W354A/D356A)* Δ*flgM*::*km* cells (Supplementary

Fig. 1). The Δ*flgM*::*km* allele restored motility of the *flhA(E351A/W354A/D356A)* mutant in a way similar to other *flgM* suppressor mutations. Then, we isolated flagella from the Δ*flgM*::*km* and *flhA(E351A/W354A/D356A)* Δ*flgM*::*km* cells and measured their hook length. The hook length of the Δ*flgM*::*km* strain was 52.0 ± 5.1 nm (mean ± SD, n = 157) (Fig. 2d), which is nearly the same as that of the wild-type strain (51.0 ± 6.9 nm)[13]. This indicates that the loss-of-function mutation of FlgM does not affect the hook length control. In contrast, the average hook length of the *flhA(E351A/W354A/D356A)* Δ*flgM*::*km* strain was 68.8 ± 30.9 nm (mean ± SD, n = 157) (Fig. 2d), indicating that the hook length control becomes worse in the presence of the E351A/W354A/D356A triple mutation. These suggest that this triple mutation affects not only the initiation of filament-type protein export but also the termination of hook-type protein export. Therefore, we propose that conformational rearrangements of $FlhA_L$ are required for well-regulated export switching of fT3SS.

Effect of FlhA linker mutations on the hydrodynamic properties of $FlhA_C$ in solution. A well conserved hydrophobic dimple of $FlhA_C$ containing Asp-456, Phe-459 and Thr-490 resides is located at the interface between domains D1 and D2 and is involved in the interactions with the FlgN, FliS and FliT chaperones in complex with their cognate filament-type substrates (Fig. 1)[15–17]. The W354A, E351A/D356A and E351A/W354A/D356A mutations significantly reduce the binding affinity of $FlhA_C$ for

these chaperone/substrate complexes[13], raising the possibility that $FlhA_L$ carrying these *flhA* mutations binds to the hydrophobic dimple of $FlhA_C$ and blocks the $FlhA_C$-chaperone interaction. If true, $FlhA_C$ with these mutations would show distinct hydrodynamic properties compared with wild-type $FlhA_C$. To clarify this possibility, we performed size exclusion chromatography with a Superdex 75 column HR 10/30 column. Wild-type His-$FlhA_C$ appeared as a single peak at an elution volume of 10.3 mL, which corresponds to the deduced molecular mass of His-$FlhA_C$ (about 43 kDa) (Fig. 3a). His-$FlhA_C$(W354A), His-$FlhA_C$(E351A/D356A) and His-$FlhA_C$(E351A/W354A/D356A) appeared as a single peak at an elution volume of 10.3 mL, 10.5 mL and 10.4 mL, respectively (Fig. 3a), indicating that these mutant variants exist as a monomer in solution. His-$FlhA_C$(E351A/D356A) exhibited a slightly delayed elution behavior compared with the wild-type. Furthermore, His-$FlhA_C$(E351A/D356A) showed a slightly faster mobility on SDS-PAGE gels. Far-UV CD measurements revealed that the E351A/D356A double mutation did not affect the secondary structures of $FlhA_C$ (Supplementary Fig. 2). These suggest that $FlhA_C$(E351A/D356A) adopts a more compact conformation than wild-type $FlhA_C$. The elution peak position of His-$FlhA_C$(E351A/W354A/D356A) was between those of the wild-type and $FlhA_C$(E351A/D356A) (Fig. 3a). Because His-$FlhA_C$(E351A/W354A/D356A) showed two different bands on SDS-PAGE gels, with a slower mobility band corresponding to wild-type $FlhA_C$ and a faster one corresponding to $FlhA_C$(E351A/D356A) (Fig. 3a, inset), we suggest that $FlhA_C$(E351A/W354A/D356A)

159 exists in an equilibrium between the wild-type conformation and the compact
160 conformation. Since $FlhA_C$(W354A) adopted the wild-type conformation (Fig. 3a), we
161 suggest that the E351A/D356A double mutation is required to make $FlhA_C$ more compact
162 and that Trp-354 of $FlhA_L$ is needed to stabilize the compact conformation.
163
164 **Effect of FlhA linker mutations on methoxypolyethylene glycol 5000 maleimide**
165 **(mPEG-maleimide) modifications of Cys-459 and Cys-548.** $FlhA_C$ structures have
166 shown that it adopts three distinct, open, semi-closed and closed
167 conformations[11,14,17,18,23]. Phe-459 and Lys-548 are fully exposed to solvent on the
168 molecular surface of the open conformation of $FlhA_C$ but are in close proximity to each
169 other in the closed conformation[11,18,23]. To test whether mutations in $FlhA_L$ bias $FlhA_C$
170 towards the closed structure, we performed Cys modification experiments with
171 mPEG-maleimide, which adds a molecular mass of ~5 kDa to a target protein.
172 $FlhA_C$(F459C/K548C) modified by mPEG-maleimide showed much slower mobility shift,
173 indicating that both Cys459 and Cys548 are exposed to the solvent. The W354A,
174 E351A/D356A and E351A/W354A/D356A mutations did not inhibit Cys modifications with
175 mPEG-maleimide at all, indicating that $FlhA_C$ with these mutations does not adopt the
176 closed conformation.
177
178 **Crystal structure of $FlhA_C$(E351A/D356A).** To investigate whether Trp-354 of $FlhA_L$

binds to the hydrophobic dimple of $FlhA_C$ to makes $FlhA_C$(E351A/D356A) more compact, we explored crystallization conditions of $FlhA_C$(E351A/D356A) for a molecular packing distinct from the open (PDB code: 3A5I)[11] and semi-closed (PDB code: 6AI0)[18] forms of wild-type $FlhA_C$. We found a new orthorhombic crystal that diffracted up to 2.8 Å resolution, with unit cell dimensions *a* = 71.7 Å, *b* = 96.2 Å, *c* = 114.1 Å (Table 1) and the asymmetric unit containing two $FlhA_C$ molecules (A and B). Mol-A adopts an open conformation similar to the 3A5I structure whereas Mol-B shows a semi-closed conformation similar to the 6AI0 structure (Supplementary Fig. 3). The residues from Val-349 to Val-357 in $FlhA_L$ of Mol-A form an α-helix, which interacts with the hydrophobic dimple of a neighboring Mol-A molecule related by a crystallographic symmetry (Fig. 4a). Trp-354 fits into the hydrophobic dimple, and Ala-351 hydrophobically contacts with Pro-442 on the periphery of the dimple (Fig. 4b). These interactions resemble the interaction between the N-terminal α-helix of FliS and the hydrophobic dimple of FlhAc (PDB ID: 6CH3)[17] (Fig. 4c). Ile-7 and Tyr-10 of the N-terminal α-helix of FliS is in the corresponding position of Ala-351 and Trp-354 of $FlhA_L$, respectively. Tyr-10 fits into the hydrophobic dimple of FlhAc, and Ile-7 interacts with Pro-442 of FlhAc (Fig. 4d). These observations suggest that $FlhA_L$ and flagellar chaperones bind competitively to a common binding site on $FlhA_C$ and that the dissociation of $FlhA_L$ from this binding site is required for the binding of the flagellar chaperones to $FlhA_C$.

Discussion

The $FlhA_C$ ring serves as the docking platform for flagellar export chaperones in complex with their cognate substrates and facilitates the export of filament-type proteins to form the filament at the hook tip after completion of hook assembly[14–17]. The $FlhA_C$ ring also ensures the strict order of flagellar protein export, thereby allowing the huge and complex flagellar structure to be built efficiently on the cell surface[13,14,16,18,19]. Interactions of $FlhA_L$ with its neighboring $FlhA_C$ subunit in the nonamer ring is required for the initiation of filament-type protein export upon completion of hook assembly. However, it remained unclear how the $FlhA_C$ ring mediates such hierarchical protein export during flagellar assembly.

In this study, we first performed genetic analyses of the *flhA(E351A/W354A/D356A)* mutant and found that the E351A/W354A/D356A triple mutation caused a loose hook-length control (Fig. 2d), indicating that the E351A/W354A/D356A mutation significantly affects the termination of hook-type protein export. Furthermore, this triple mutation also reduced the secretion levels of the filament-type proteins considerably (Fig. 2b), thereby reducing the number of flagellar filaments per cell (Fig. 2c). These results suggest that $FlhA_L$ serves as a structural switch for substrate specificity switching of fT3SS from hook-type to filament-type and that Glu-351, Trp-354 and Asp-356 of $FlhA_L$ are directly involved in this export switching mechanism.

It has been reported that the W354A, E351A/D356A and E351A/W354A/D356A mutations inhibit interactions between $FlhA_C$ and flagellar chaperones in complex with their cognate filament-type substrates[13], suggesting that $FlhA_L$ regulates the binding of flagellar chaperones to $FlhA_C$. The crystal structure of $FlhA_C$(E351A/D356A) showed that Trp-354 of one Mol-A molecule bound to the hydrophobic dimple of the flagellar chaperone binding site of its nearest Mol-A in the crystal (Fig. 4). Although the relative orientations of these Mol-A molecules in the crystal differs from those in the $FlhA_C$ nonameric ring, $FlhA_L$ can bind to the hydrophobic dimple of $FlhA_C$ in the nonamer ring structure because of a highly flexible nature of $FlhA_L$ (Fig. 5). The C-terminal region of $FlhA_L$ is flexible enough to allow such subunit orientations without changing the essential interaction between $FlhA_L$ and the chaperone binding site of $FlhA_C$, as it has been shown to have various conformations in the known FlhAc structures[18]. Therefore, we propose that an interaction between $FlhA_L$ and the hydrophobic dimple of its neighboring $FlhA_C$ subunit suppresses the docking of flagellar chaperones to the $FlhA_C$ ring platform during HBB assembly and that the hook completion induces the detachment of $FlhA_L$ from the dimple through an interaction between $FliK_C$ and $FlhB_C$ and its attachment to the D1 and D3 domains to induce structural remodeling of the $FlhA_C$ ring, thereby terminating hook assembly and initiating filament formation (Fig. 5). Because Trp-354 of $FlhA_L$ stabilized a more compact conformation of the $FlhA_C$(E351A/D356A) monomer compared to the wild-type $FlhA_C$ and $FlhA_C$(W354A) monomers (Fig. 3), it is also possible that $FlhA_L$ may

239 block the docking of the flagellar chaperones to $FlhA_C$ by covering the binding site of the
240 same $FlhA_C$ molecule.
241

242 ## Methods

243 **Bacterial strains and plasmids.** Bacterial strains and plasmids used in this study are
244 listed in Supplementary Table 1.
245

246 **DNA manipulations.** DNA manipulations and site-directed mutagenesis were carried out
247 as described previously[24]. DNA sequencing reactions were carried out using BigDye v3.1
248 (Applied Biosystems) and then the reaction mixtures were analyzed by a 3130 Genetic
249 Analyzer (Applied Biosystems).
250

251 **Motility assays.** Fresh colonies were inoculated into soft agar plates [1% (w/v) triptone,
252 0.5% (w/v) NaCl, 0.35% Bacto agar] and incubated at 30°C.
253

254 **Secretion assays.** Details of sample preparations have been described previously[25].
255 After SDS-polyacrylamide gel electrophoresis (PAGE), immunoblotting with polyclonal
256 anti-FlgD, anti-FlgE, anti-FlgK, or anti-FliD antibody was carried out as described
257 previously[26].

Hook length measurements. The HBBs were purified from NH004gM carrying pMM130 or pYI003 as described previously[27]. The HBBs were negatively stained with 2%(w/v) uranyl acetate. Electron micrographs were recorded with a JEM-1011 transmission electron microscope (JEOL, Tokyo, Japan) operated at 100 kV and equipped with a F415 CCD camera (TVIPS, Gauting, Germany). Hook length was measured by ImageJ version 1.48 (National Institutes of Health).

Protein purification. *E. coli* BL21 (DE) Star cells carrying a pET15b-based plasmid encoding His-FlhA$_C$ or its mutant variants were grown overnight at 30ºC in 250 mL of L-broth [1% (w/v) tryptone, 0.5% (w/v) yeast extract, 0.5% (w/v) NaCl] containing ampicillin. His-FlhA$_C$ and its mutant variants were purified by affinity chromatography, followed by size exclusion chromatography as described previously[24].

Far-UV CD spectroscopy. Far-UV CD spectroscopy of His-FlhA$_C$ or its mutant variants was carried out at room temperature using a Jasco-720 spectropolarimeter (JASCO International Co., Tokyo, Japan) as described previously[28].

Cystein modification by mPEG-maleimide. His-FlhA$_C$(F459C), His-FlhA$_C$(K548C), His-FlhA$_C$(F459C/K548C), His-FlhA$_C$(W354A/F459C/K548C),

His-FlhA$_C$(E351A/D356A/F459C/K548C) and His-FlhA$_C$(E351A/W354A/D356A/F459C/K548C) were dialyzed overnight against PBS (8 g of NaCl, 0.2 g of KCl, 3.63 g of Na_2HPO_4 $12H_2O$, 0.24 g of KH_2PO_4, pH 7.4 per liter) at 4ºC, followed by cysteine modification by mPEG-maleimide (Fluka) as described previously[18]. Each protein solution was run on SDS-PAGE and then analyzed by Coomassie Brilliant blue (CBB) staining.

X-ray crystallographic study of FlhA$_C$(E351A/D356A). Initial crystallization screening was performed at 20°C by the sitting-drop vapor-diffusion method using Wizard Classic I and II, Wizard Cryo I and II (Rigaku Reagents, Inc.), Crystal Screen and Crystal Screen 2 (Hampton Research). Crystals suitable for X-ray analysis were obtained from drops prepared by mixing 0.5 µL protein solution with 0.5 µL reservoir solution containing 0.1 M Tris-HCl (pH 8.5), 20% (v/v) PEG 8000, and 200 mM $MgCl_2$. X-ray diffraction data were collected at synchrotron beamline BL41XU in SPring-8 (Harima, Japan) with the approval of the Japan Synchrotron Radiation Research Institute (JASRI) (Proposal No. 2016B2544 and 2018A2568). The FlhA$_C$(E351A/D356A) crystal was soaked in a solution containing 90% (v/v) of the reservoir solution and 10% (v/v) glycerol for a few seconds and was directly transferred into liquid nitrogen for freezing. The X-ray diffraction data were collected under nitrogen gas flow at 100 K. The diffraction data were processed

297 with MOSFLM[29] and were scaled with Aimless[30]. The initial phase was determined by
298 molecular replacement using the software package Phenix[31] with the wild-type $FlhA_C$
299 structure in the orthorhombic crystal form (PDB code: 6AI0) as a search model. The
300 atomic model was constructed with COOT[32] and refined with Phenix[31]. During the
301 refinement process, iterative manual modification was performed. The diffraction data
302 statistics and refinement statistics are summarized in Table 1.

303

304 Accession code

305 The atomic coordinates have been deposited in Protein Data Bank under the accession
306 code 7CTN.

307

308 References

309 1. Minamino, T., Kawamoto, A., Kinoshita, M. & Namba, K. Molecular organization and
310 assembly of the export apparatus of flagellar type III secretion systems. *Curr. Top*
311 *Microbiol. Immunol.* **427**, 91–107 (2020).
312 2. Minamino, T. Hierarchical protein export mechanism of the bacterial flagellar type III
313 protein export apparatus. *FEMS Microbiol. lett.* **365**, fny117 (2018).
314 3. Terashima, H. *et al. In vitro* reconstitution of functional type III protein export and
315 insights into flagellar assembly. *mBio* **9**, e00988-18 (2018).

4. Terashima, H. *et al*. *In vitro* autonomous construction of the flagellar axial structure in the inverted membrane vesicles. *Biomolecules* **10**, 126 (2020).

5. Minamino, T., González-Pedrajo, B., Yamaguchi, K., Aizawa, S.-I. & Macnab, R. M. FliK, the protein responsible for flagellar hook length control in *Salmonella*, is exported during hook assembly. *Mol. Microbiol.* **34**, 295–304 (1999).

6. Moriya, N., Minamino, T., Hughes, K. T., Macnab, R. M. & Namba, K. The type III flagellar export specificity switch is dependent on FliK ruler and a molecular clock. *J. Mol. Biol.* **359**, 466–477 (2006).

7. Shibata, S., *et al*. (2007) FliK regulates flagellar hook length as an internal ruler. *Mol. Microbiol.* **64**, 1404–1415.

8. Erhardt, M., Singer, H. M., Wee, D. H., Keener, J. P. & Hughes, K.T. An infrequent molecular ruler controls flagellar hook length in *Salmonella enterica. EMBO J.* **30**, 2948–2961 (2011).

9. Kinoshita, M., Aizawa, S.I., Inoue, Y., Namba, K. & Minamino, T. The role of intrinsically disordered C-terminal region of FliK in substrate specificity switching of the bacterial flagellar type III export apparatus. *Mol. Microbiol.* **105**, 572–588 (2017).

10. Kinoshita, M., Tanaka, S., Y. Inoue, Y., Namba, K. Aizawa, S.I. & Minamino, T. The flexible linker of the secreted FliK ruler is required for export switching of the flagellar protein export apparatus. *Sci. Rep.* **10**, 838 (2020).

11. Saijo-Hamano, Y. *et al*. Structure of the cytoplasmic domain of FlhA and implication

for flagellar type III protein export. *Mol. Microbiol.* **76**, 260–268 (2010).

12. Abrusci, P. *et al*. Architecture of the major component of the type III secretion system export apparatus. *Nat. Struct. Mol. Biol.* **20**, 99–104 (2013).
13. Terahara, N. *et al.* Insight into structural remodeling of the FlhA ring responsible for bacterial flagellar type III protein export. *Sci. Adv.* **4**, eaao7054 (2018).
14. Bange G. *et al*. FlhA provides the adaptor for coordinated delivery of late flagella building blocks to the type III secretion system. *Proc. Natl. Acad. Sci. USA* **107**, 11295–11300 (2010).
15. Minamino, T. *et al*. Interaction of a bacterial flagellar chaperone FlgN with FlhA is required for efficient export of its cognate substrates. *Mol. Microbiol.* **83**, 775–788 (2012).
16. Kinoshita, M., Hara, N., Imada, K., Namba, K. & Minamino, T. Interactions of bacterial chaperone-substrate complexes with FlhA contribute to co-ordinating assembly of the flagellar filament. *Mol. Microbiol.* **90**, 1249–1261 (2013).
17. Xing, Q. *et al*. Structure of chaperone-substrate complexes docked onto the export gate in a type III secretion system. *Nat. Commun*. **9**, 1773 (2018).
18. Inoue, Y. *et al*. Structural insight into the substrate specificity switching mechanism of the type III protein export apparatus. *Structure* **27**, 965–976 (2019).
19. Minamino, T., Inoue, Y., Kinoshita, M. & Namba, K. FliK-driven conformational rearrangements of FlhA and FlhB are required for export switching of the flagellar

356 protein export apparatus. *J. Bacteriol.* **202,** e00637-19 (2020).

357 20. Gillen, K.L. & K.T. Hughes. Molecular characterization of *flgM*, a gene encoding a
358 negative regulator of flagellin synthesis in *Salmonella typhimurium*. *J. Bacteriol.* **173**,
359 6453–6459 (1991).

360 21. Erhardt, M., Mertens, M.E., Fabiani, F.D. & Hughes, K.T. ATPase-independent
361 type-III protein secretion in *Salmonella enterica*. *PLoS Genet.* **10**, e1004800 (2014).

362 22. Minamino, T., Morimoto, Y.V., Hara, N. & Namba, K. An energy transduction
363 mechanism used in bacterial type III protein export. *Nat. Commun.* **2**, 475 (2011).

364 23. Moore, S.A., and Jia, Y. Structure of the cytoplasmic domain of the flagellar secretion
365 apparatus component FlhA from *Helicobacter pylori*. *J. Biol. Chem.* **285**, 21060–
366 21069 (2010).

367 24. Saijo-Hamano, Y., Minamino, T., Macnab, R.M. & Namba, K. Structural and functional
368 analysis of the C-terminal cytoplasmic domain of FlhA, an integral membrane
369 component of the type III flagellar protein export apparatus in *Salmonella*. *J. Mol. Biol.*
370 **343**, 457-466 (2004).

371 25. Minamino, T., Kinoshita, M. & Namba, K. Fuel of the bacterial flagellar type III protein
372 export apparatus. *Methods Mol. Biol.* **1593**, 3–16 (2017).

373 26. Minamino, T. & Macnab, R. M. Components of the *Salmonella* flagellar export
374 apparatus and classification of export substrates. *J. Bacteriol.* **181**, 1388–1394
375 (1999).

376 27. Inoue, Y., Morimoto, Y. V., Namba, K. & Minamino, T. Novel insights into the
377 mechanism of well-ordered assembly of bacterial flagellar proteins in *Salmonella*. *Sci.*
378 *Rep*. **8**, 1787 (2018).
379 28. Shimada, M. *et al*. Functional defect and restoration of temperature-sensitive
380 mutants of FlhA, a subunit of the flagellar protein export apparatus. *J. Mol. Biol.* **415**,
381 855–865 (2012).
382 29. Battye, T.G., Kontogiannis, L., Johnson, O., Powell, H.R. & Leslie, A.G. 'iMOSFLM: a
383 new graphical interface for diffraction-image processing with MOSFLM'. *Acta*
384 *Crystallogr. D Biol. Crystallogr*. **67**, 271–281 (2011).
385 30. Evans, P.R. & Murshudov, G.N. How good are my data and what is the resoluton?
386 *Acta Crystallogr. D Biol. Crystallogr.* **69**, 1204–1214 (2013).
387 31. Adams, P.D., *et al.* PHENIX: a comprehensive Python-based system
388 formacromolecular structure solution. *Acta Crystallogr. D Biol. Crystallogr.* **66**, 213–
389 221 (2010).
390 32. Emsley, P., Lohkamp, B., Scott, W.G. & Cowtan, K. Features and development of
391 Coot. *Acta Crystallogr. D Biol. Crystallogr.* **66**, 486–501 (2010).

392

393 ## Acknowledgements

394 We thank beamline staffs at SPring-8 for technical help in use of beamlines BL41XU.
395 This work was supported in part by JSPS KAKENHI Grant Numbers JP18K14638 and

396 JP20K15749 (to M.K.), JP16J01859 (to N.T.), 25000013 (to K.N.), 15H02386 (to K.I.) and
397 JP26293097 and JP19H03182 (to T.M.). This work has also been partially supported by
398 JEOL YOKOGUSHI Research Alliance Laboratories of Osaka University to K.N.

399

400 Author Contributions

401 K.N. K.I. and T.M. conceived and designed research; Y.I., M.Kida, M.Kinoshita, N.T., K.I.
402 and T.M. preformed research; Y.I., M.Kida, M.Kinoshita, N.T., K.I. and T.M. analysed the
403 data; and K.N., K.I. and T.M. wrote the paper based on discussion with other authors.

404

405 Competing interests

406 The authors declare no competing interests.

407

408 Data availability

409 All data generated during this study are included in this published article and its
410 Supplementary Information files.

411 **Table 1. X-ray data collection and refinement statistics**

X-ray data collection		
Space group	$P2_12_12_1$	
Cell dimensions *a, b, c* (Å)	71.7, 96.2, 114.1	
Wavelength (Å)	1.0000	
Resolution (Å)	73.5-2.80	(2.95-2.80)
R_{merge}	0.074	(0.317)
R_{pim}	0.065	(0.283)
CC(1/2)	0.995	0.915
$I/\sigma I$	8.1	(2.8)
Completeness (%)	97.1	(94.6)
Redundancy	3.4	(3.1)
Refinement statistics		
Resolution range (Å)	73.5-2.80	(2.87-2.80)
No. of reflections working	17,398	(1,182)
No. of reflections test	1,903	(112)
R_w (%)	23.2	(33.5)
R_{free} (%)	29.0	(42.1)
Rms deviation bond length (Å)	0.003	
Rms deviation Bond angle (°)	0.680	
B-factors Protein atoms Solvent atoms	 70.0 -	
Ramachandran plot (%) Most favored Allowed Disallowed	 96.0 3.9 0.1	
No. of protein atoms	5, 252	
No. of solvent atoms	0	

412

413 Values in parentheses are for the highest resolution shell.

414 $R_w = \sum || Fo | - | Fc || / \sum | Fo |$, $R_{free} = \sum || Fo | - | Fc || / \sum | Fo |$

415

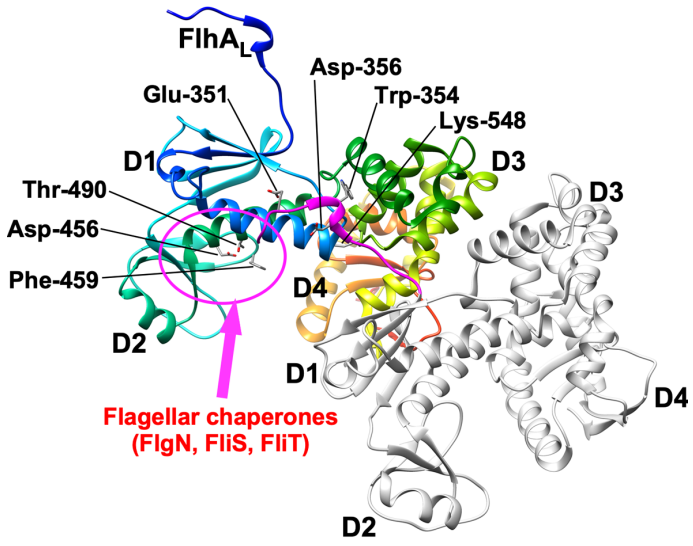

Fig. 1. FlhA$_C$ structure in a crystal (PDB ID: 3A5I). FlhA$_C$ consists of four domains, D1, D2, D3 and D4 and a flexible linker (FlhA$_L$). Glu-351, Trp-354 and Asp-356 of FlhA$_L$ binds to the D1 and D3 domains of its neighboring subunit. A well-conserved hydrophobic dimple including Phe-459 is responsible for the interaction of FlhA$_C$ with flagellar export chaperones in complex with filament-type substrates. Phe-459 and Lys-548 are exposed to solvent on the molecular surface when FlhA$_C$ adopts the open conformation. The interactions between the two FlhA$_C$ molecules in this crystal also represent those in the FlhA$_C$ nonameric ring of the export apparatus.

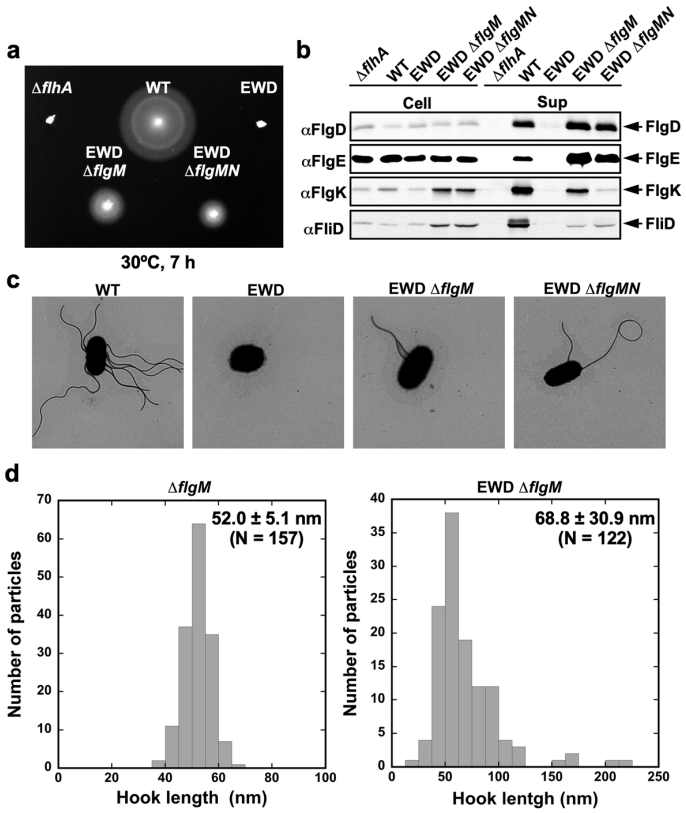

Fig. 2. Isolation pseudorevertants from the *flhA(E351A/W354A/D356A)* mutant. (a) Motility of the *Salmonella* NH001 strain transformed with pTrc99A (Δ*flhA*), pMM130 (WT), or pYI003 [FlhA(E351A/W354A/D356A) indicated as EWD]), YI1003-4 (EWD Δ*flgM*) or YI1003-13 (EWD Δ*flgMN*) in soft agar. (b) Immunoblotting using polyclonal anti-FlgD (1st row), anti-FlgE (2nd row), anti-FlgK (3rd row) or anti-FliD (4th row) antibody, of whole cell proteins (Cell) and culture supernatants (Sup) prepared from the above strains. (c) Electron micrographs of the above cells. (d) Histogram of hook length distribution of NH001gM (Δ*flhA* Δ*flgM*::*km*) carrying pMM130 (Δ*flgM*) or pYI003 (EWD Δ*flgM*).

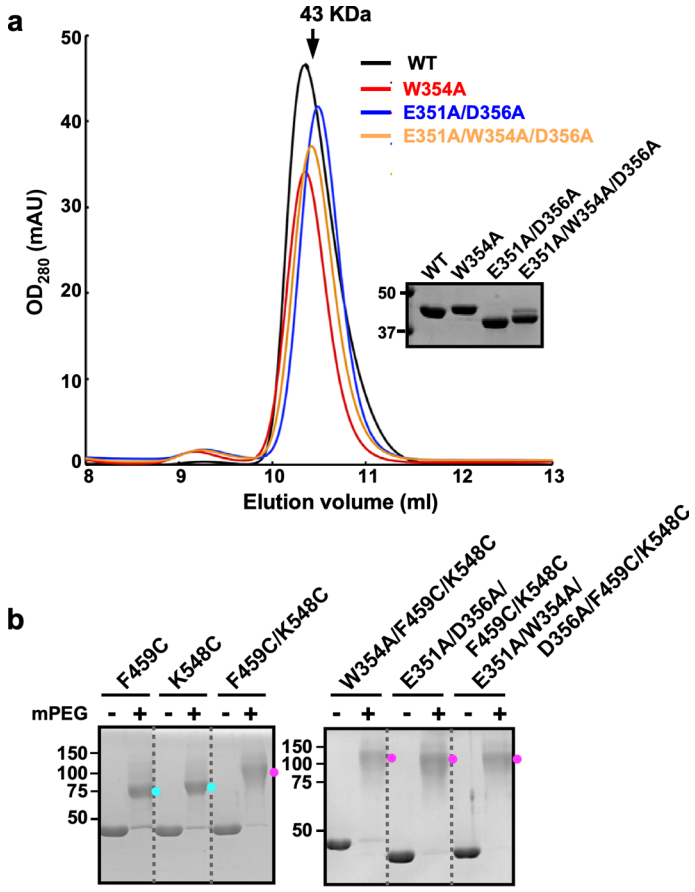

Fig. 3. Effect of FlhA linker mutations on the FlhA$_C$ conformation. (a) Size exclusion chromatography using a Superdex 75HR 10/30 column. Elution positions of His-FlhA$_C$ (WT, black), His-FlhA$_C$(W354A) (red), His-FlhA$_C$(E351A/D356A) (blue) and His-FlhA$_C$(E351A/W354A/D356A) (orange) are 10.3 ml, 10.3 ml, 10.5 ml and 10.4 ml, respectively. Arrow indicates the elution peak of ovalbumin (43 kDa). Inset, CBB-stained gels of purified FlhA$_C$ proteins. (b) Effect of FlhA mutations on mPEG-maleimide modification of Cys459 and Cys548. His-FlhA$_C$(F459C), His-FlhA$_C$(K548C), His-FlhA$_C$(F459C/K548C), His-FlhA$_C$(W354A/F459C/K548C), His-FlhA$_C$(E351A/D356A/F459C/K548C) and His-FlhA$_C$(E351A/W354A/D356A/F459C/K548C) were incubated with (+) or without (-) mPEG-maleimide. After centrifugation at 20,000 g for 20 min to remove any aggregates, supernatants were analyzed by SDS-PAGE with CBB staining. Cyan and magenta dots indicate positions of FlhA$_C$-(mPEG) and FlhA$_C$-(mPEG)$_2$, respectively.

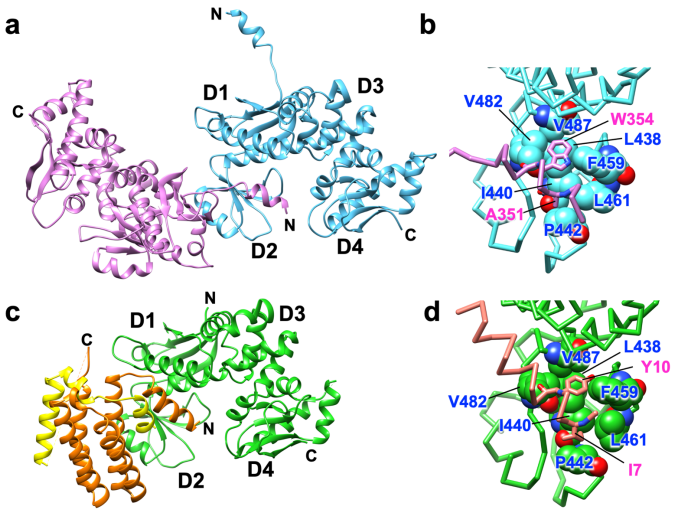

Fig. 4. Interaction between $FlhA_L$ and a well conserved hydrophobic dimple of its neighboring $FlhA_C$ in the crystal of $FlhA_C$(E351A/D356A). (a) Mol-A of $FlhA_C$(E351A/D356A) (magenta) interacts with neighboring Mol-A (cyan) related by a crystallographic symmetry. (b) Close-up view of the interaction between $FlhA_L$ and the hydrophobic dimple. Residues that form the hydrophobic dimple are indicated by balls. Ala-351 and Trp-354 in $FlhA_L$ are shown in stick models. (c) Interaction between $FlhA_C$ (green) and FliS (orange) fused with the C-terminal region of FliC (yellow) (PDB code: 6CH3). (d) Close-up view of the interaction between FliS and the hydrophobic dimple. The residues that form the hydrophobic dimple are indicated by ball. Ile-7 and Tyr-10 of FliS are shown in stick models.

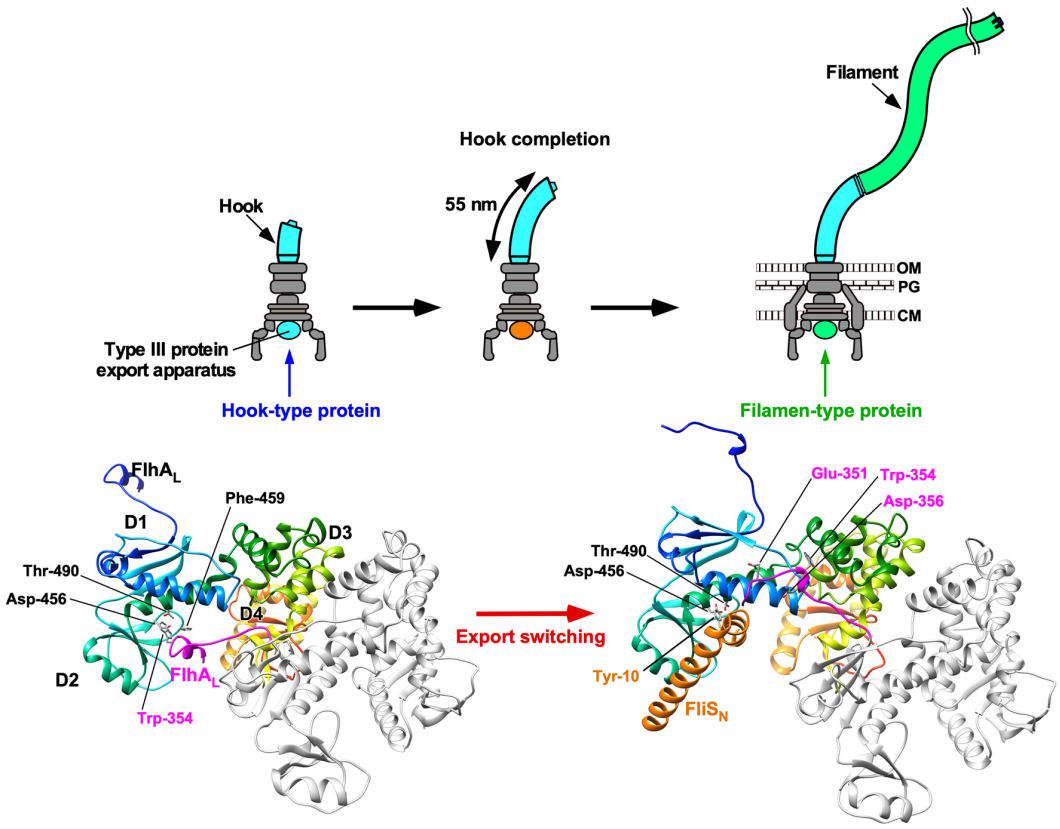

Fig. 5. Structural rearrangements of FlhA$_L$ responsible for export switching of fT3SS. Trp-359 of FlhA$_L$ binds to a well-conserved hydrophobic dimple containing Asp-456, Phe-459 and Thr-490 of its neighboring FlhA$_C$ subunit in the FlhA$_C$ ring to inhibit the interaction of FlhA$_C$ with flagellar chaperones in complex with their cognate filament-type substrates during hook assembly. When the hook reaches its mature length of about 55 nm, an interaction between FliK$_C$ and FlhB$_C$ triggers a conformational rearrangement of the FlhA$_C$ ring so that FlhA$_L$ dissociates from the hydrophobic dimple and binds to the D1 and D3 domains of the neighboring FlhA$_C$ subunit, allowing the chaperones to bind to FlhA$_C$ to facilitate the export of their cognate substrates for filament assembly.